JOC Article

On the Surface-Catalyzed Reaction between the Gases 2,2-Dimethylpropanal and Methanamine. Formation of Active-Site Imines

Linda M. Mascavage,[†] Philip E. Sonnet,[‡] and David R. Dalton*,[‡]

Department of Chemistry, Arcadia University, Glenside, Pennsylvania 19038, and Department of Chemistry, Temple University, Philadelphia, Pennsylvania 19122

david.dalton@temple.edu

Received December 5, 2005

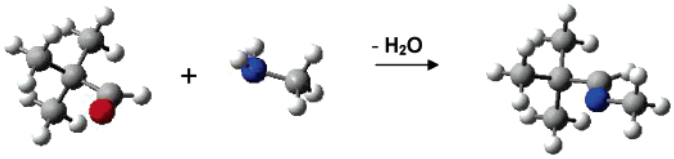

The reaction that occurs when vapors of 2,2-dimethylpropanal and methanamine are allowed to mix in an infrared gas cell has been examined. The disappearance of starting materials and formation of *E*-imine product, monitored simultaneously, is best fit by a process involving wall-associated water. The same or closely related processes have been successfully modeled; such processes may also be common to pyridoxal-catalyzed transamination and related reactions in biological systems.

Introduction

In 1864, Schiff,[1] following more than a decade after the early work of Laurent and Gerhardt,[2] described the formation of products resulting from the condensation of amines and aldehydes. Schiff identified **imines**, compounds containing a carbon-to-nitrogen double bond, and **1,1-diamines** in his report. The latter apparently resulted from the addition of a second equivalent of amine across the carbon−nitrogen double bond of the initially formed imine. Subsequently, both imines (now called "Schiff bases") and 1,1-diamines have been studied intensively,[3] and work in the last several decades has implicated both imines and 1,1-diamines in biological processes, including pyridoxal (vitamin B_6)-catalyzed reactions such as transamination.[3e,4]

The efforts to understand the details of the Schiff process, which include some kinetic studies, have led to the generally accepted pathway for the solution reaction as shown in Scheme 1[5] where, shorn of its intimate details, the current picture is broadly drawn. The accepted pathway to imine proceeds through a carbinolamine (and/or its conjugate acid/base) and the latter loses water. The hydrolysis of imines is, of course, the microscopic reverse.

A more thorough kinetic investigation of the reaction in the gas phase was envisioned in which methanamine (MA) and acetaldehyde (AA) were the reactants, but this reaction was complicated by competing condensations. However, we found that 2,2-dimethylpropanal [$(CH_3)_3CCHO$, pivaldehyde, PA] was suitable, and we report here both our studies on the reaction of this aldehyde with methanamine [CH_3NH_2, methylamine, MA] when these are mixed as gases and an evaluation of the same system using computational methods.[7] We conclude with some

[†] Arcadia University.
[‡] Temple University.

(1) Schiff, H. *Ann. Chem. Pharm.* **1864**, 118.
(2) Laurent, L. H.; Gerhardt, C. *Liebigs Ann. Chem.* **1850**, *76*, 304.
(3) Numerous compendia have discussions of these studies. Some of the more inclusive can be found in: (a) *The Chemistry of the Carbon−nitrogen Double Bond*; Patai, S., Ed.; Interscience: New York, 1970. (b) *The Chemistry of the Double-Bonded Functional Groups*; Patai, S., Ed.; Interscience: New York, 1977; Parts 1 and 2; (c) ibid. Supplement A3, Parts 1 and 2, 1997. (d) Söll, H. In *Methoden der Organischen Chemie (Houben-Weyl)*, 4th ed.; Müller, G., Ed.; Georg Thieme Verlag: Stuttgart, 1958; Vol. 11/2, p 73 ff. (e) Tehrani, K. A.; DeKimpe, N. In *Science of Synthesis, Houben-Weyl*; Padwa, A., Ed.; Georg Thieme Verlag: New York, 2004; Vol. 4/27, p 245 ff.
(4) Giuseppone, N.; Schmitt, J.-L.; Schwartz, E.; Lehn, J.-M. *J. Am. Chem. Soc.* **2005**, *127*, 5528 and references therein.
(5) Sayer, J. M.; Conlon, P. *J. Am. Chem. Soc.* **1980**, *102*, 3592 and references therein.
(6) Bürgi, H. B.; Dunitz, J. D.; Shefter, E. *J. Am. Chem. Soc.* **1973**, *95*, 5065.
(7) Frisch, M. J.; Trucks, G. W.; Schlegel, H. B.; Scuseria, G. E.; Robb, M. A.; Cheeseman, J. R.; Zakrzewski, V. G.; Montgomery, J. A., Jr.; Stratmann, R. E.; Burant, J. C.; Dapprich, S.; Millam, J. M.; Daniels, A. D.; Kudin, K. N.; Strain, M. C.; Farkas, O.; Tomasi, J.; Barone, V.; Cossi, M.; Cammi, R.; Mennucci, B.; Pomelli, C.; Adamo, C.; Clifford, S.; Ochterski, J.; Petersson, G. A.; Ayala, P. Y.; Cui, Q.; Morokuma, K.; Malick, D. K.; Rabuck, A. D.; Raghavachari, K.; Foresman, J. B.; Cioslowski, J.; Ortiz, J. V.; Stefanov, B. B.; Liu, G.; Liashenko, A.; Piskorz, P.; Komaromi,

10.1021/jo052503z CCC: $33.50
Published on Web 03/30/2006

SCHEME 1. Generic Cartoon Representation of a Series of Species Expected To Lie between Carbonyl (Aldehyde/Ketone) and Amine Reactants and Imine and Water Products (in the Forward Direction)[a]

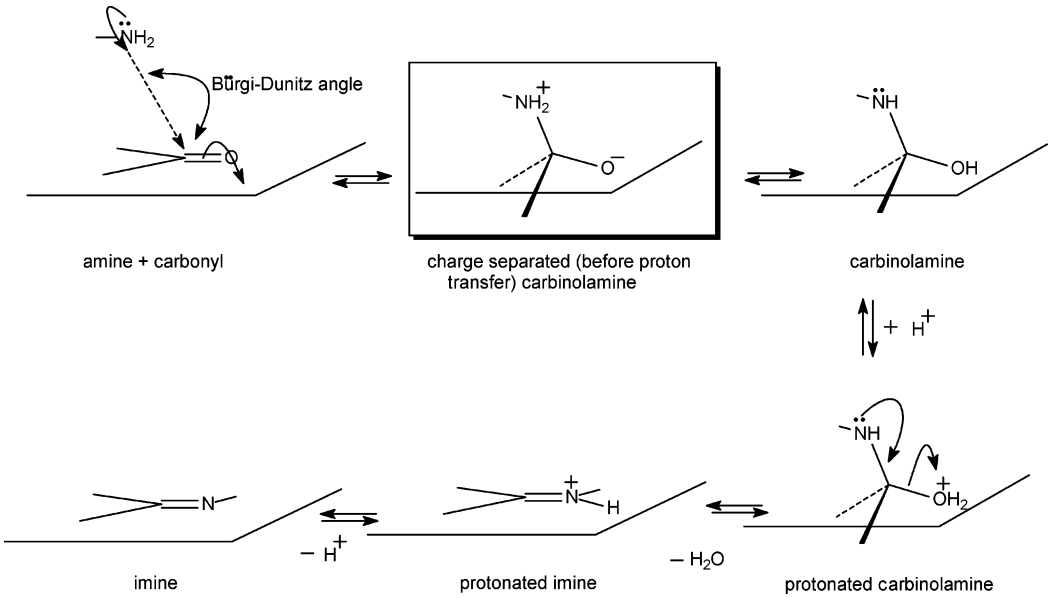

[a] In principle (and in practice), the process can proceed in either direction and the "Bürgi-Dunitz" angle[6] is expected to obtain.

suggestions regarding pyridoxal-mediated enzymatic processes that result from extension of our findings to the wealth of information extant in the protein data bank (PDB).[8]

Computations specific for the reaction of simple amines and aldehydes were viewed as a natural adjunct to the experiments performed here and do not appear to have been reported previously. Computational work on related systems, such as ammonia and water additions to methanal (formaldehyde), indicated diminished energies of activation when the incipient charged species was associated with one or more additional water molecules (HF/3-21G and AM1 levels).[9] More recently, reaction of ammonia with methyl formate was evaluated (QCISD/6-31G(d) and B3LYP/6-31G(d)).[10] The addition step, involving ammonia and the formate ester, as well as the subsequent elimination step, giving methanol and formamide, exhibited lower barriers if conducted with an additional ammonia molecule. In like manner, aminolysis of oxo- and thioesters was found to favor stepwise mechanisms, each augmented by an additional water molecule (B3LYP/6-31G(d)).[11] Finally, gas-phase hydrazone formation was optimal with an additional molecule of hydrazine incorporated in a cyclic addition mechanism.[12]

Thus, we report our calculations for the reactions of MA with PA to: (1) examine the (generic) nature of additions of amines to aldehydes and the subsequent dehydration of the initially formed carbinolamine with additional water/amine molecule(s); (2) compare the computational results with those derived from the (experimental) reaction between the gases MA and PA; and (3) assess the implications for the analogous biological addition−elimination reactions. We also note that the computational data would allow comparisons with the Burgi−Dunitz approach angle for the condensation step and assessments of the departure angles for the elimination step, as well as dihedral angles that serve as criteria for definition of the elimination reactions as *syn* or *anti* processes.

Experimental Results and Discussion

Typical FT-IR absorbance spectra (eight scans) of a reaction mixture (at 296 K) originally containing 19.9 Torr of gaseous 2,2-dimethylpropanal (pivaldehyde, PA) and 21.3 Torr of gaseous methanamine (methylamine, MA) in a Pyrex cell immediately after mixing and at ca.7 min later, respectively, are provided in the Supporting Information as Figure S1. Unique characteristic absorbances, chosen for preparation of Beer's Law plots and subsequent analysis, were followed simultaneously and could be assigned to PA (2720.0−2661.0 cm^{-1} and 1782.9−1726.06 cm^{-1}), to 2,2-dimethylpropanal methanimine (pivaldimine, PI) (1699.7−1664.8 cm^{-1}), and to MA (1091.0−1063.3 cm^{-1}).[13,14]

Although no peaks above background noise could be detected that might be attributed to other than those of the starting materials and imine product in the infrared spectra, both gaseous and condensed (liquid nitrogen) reaction mixtures were, on completion of the reaction, transferred to NMR tubes via a vacuum rack and spectra acquired. No product other than imine was detected.

Plots of disappearance of PA and MA and appearance of PI, derived from a series of spectra intermediate to those represented by the spectra in Figure S1 (i.e., originally 19.9 Torr in PA and

I.; Gomperts, R.; Martin, R. L.; Fox, D. J.; Keith, T.; Al-Laham, M. A.; Peng, C. Y.; Nanayakkara, A.; Gonzalez, C.; Challacombe, M.; Gill, P. M. W.; Johnson, B. G.; Chen, W.; Wong, M. W.; Andres, J. L.; Head-Gordon, M.; Replogle, E. S.; Pople, J. A. *Gaussian 98*, revision A.7; Gaussian, Inc.: Pittsburgh, PA, 1998.

(8) http://www.wwpdb.org/.

(9) (a) Williams, I. H.; Spangler, D.; Femec, D. A.; Maggiora, D. M. *J. Am. Chem. Soc.* **1983**, *105*, 31. (b) Williams, I. H. *J. Am. Chem. Soc.* **1987**, *109*, 6299.

(10) Ilieva, S.; Galabov, B.; Musaev, D. G.; Morokuma, K.; Schaefer, H. F., III. *J. Org. Chem.* **2003**, *68*, 1496.

(11) Yang, W.; Drueckhammer, D. G. *J. Am. Chem. Soc.* **2001**, *123*, 11004.

(12) Custer, T. G.; Kato, S.; Bierbaum, V. M.; Howard, C. J.; Morrison, G. C. *J. Am. Chem. Soc.* **2004**, *126*, 2744.

(13) Quast, H.; Kees, F. *Chem. Ber.* **1981**, *114*, 774.

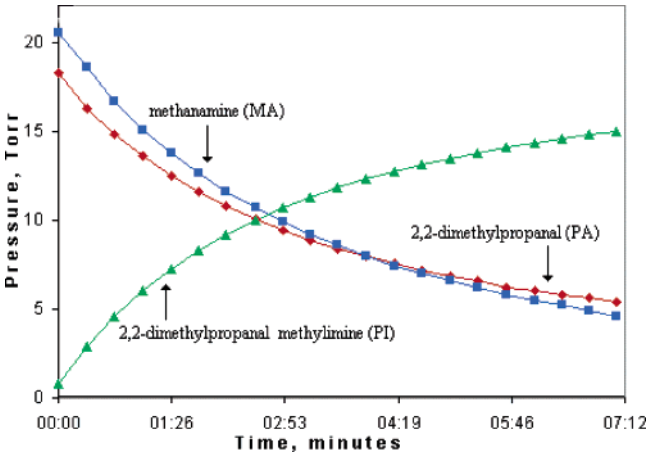

FIGURE 1. Representation of the disappearance of 2,2-dimethylpropanal (PA, ♦) and methanamine (MA, ■) and appearance of the corresponding 2,2-dimethylpropanal methylimine (PI, ▲) product, as a function of time. Pressures were calculated by measuring peak areas, derived from Beer's Law plots, found in a series of spectra intermediate to those shown in Figure S1 (Supporting Information) (i.e., originally 19.9 Torr in PA and 21.3 Torr in MA).

21.3 Torr in MA), are shown in Figure 1. Initial rates were determined from the initial slopes of these plots.

Table 1 presents a portion of the large volume of typical initial rate data at 296 K we have collected for the PA−MA system using various initial pressures of each gas in various IR cells (vide infra).

Table 2 presents the data for the same reaction in variable-temperature Pyrex cells initially containing 19.7 ± 0.8 Torr of PA and 203 ± 3 Torr of MA at reaction temperatures of 283, 294, and 331 K. The overall rates for the disappearance of both reactants and for the appearance of the product exhibited only a small temperature dependence. Over the limited temperature range examined, the disappearance of PA occurs with an apparent E_a of 2.66 kcal mol^{-1}, a $\Delta H^{\ddagger}_{294}$ of 5.23 kcal mol^{-1}, and a $\Delta S^{\ddagger}_{294}$ of −68.99 eu mol; the disappearance of MA occurs with an apparent E_a of 3.92 kcal mol^{-1}, a $\Delta H^{\ddagger}_{294}$ of 6.09 kcal mol^{-1}, and a $\Delta S^{\ddagger}_{294}$ of −68.47 eu mol; and the appearance of PI occurs with an apparent E_a of 4.16 kcal mol^{-1}, a $\Delta H^{\ddagger}_{294}$ of 8.98 kcal mol^{-1}, and a $\Delta S^{\ddagger}_{294}$ of −70.55 eu mol. Reactions which fail to show a normal temperature dependence are frequently found to be wall or surface catalyzed. Therefore, as it appears that the process we observe is wall catalyzed (vide infra), the exact significance of these numbers is not clear, although they are suggestive of a very highly ordered transition state which, in this case, may be wall associated.

To evaluate the effects of walls and added surface, the surface area of the Pyrex reaction vessels was varied through the addition of coarse porosity Pyrex fritted disks, with surface-to-volume ratios increasing about 20-fold.[15] For initial pressures of PA and MA of 20 Torr each, Figure 2 demonstrates that, at 295 K, the initial rates for the disappearance of both PA and MA, i.e., (−d[PA]/dt) and (−d[MA]/dt), are proportional to the surface-to-volume ratio of the cell. In proportion to added

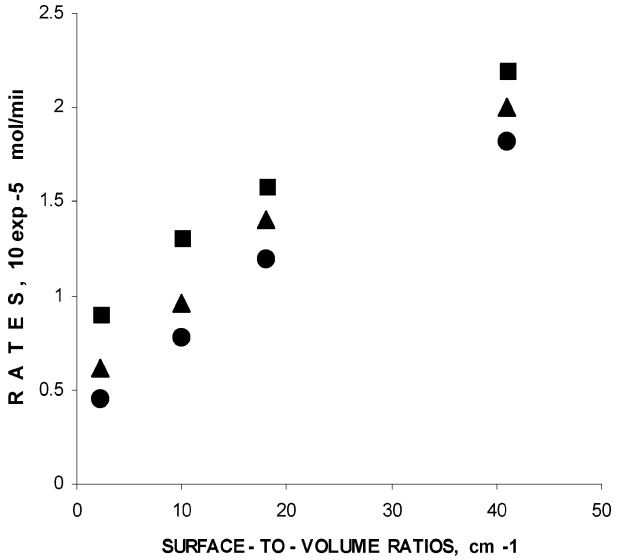

FIGURE 2. Variation in the initial rates of disappearance (rate^0) of 2,2-dimethylpropanal$_{(g)}$[a] (pivaldehyde, PA; ●) and methanamine$_{(g)}$ (methylamine, MA; ▲) and the appearance of 2,2-dimethylpropanal methylimine$_{(g)}$ (PI; ■) as a function of the surface-to-volume ratio (S/V) at 295 K in Pyrex IR cells with sidearm. The initial concentrations of PA (●) and MA (▲) were 20 ± 1 Torr ((2.26 ± 0.15) × 10^{-5} mol).[b] [a]The reaction of PA was followed in both the C−H and C═O regions (2720.0−2661.0 and 1782.9−1726.06 cm^{-1}, respectively). Results are within ±1% agreement. The data in the figure are for the C═O region. [b]Data points are the average of at least two (2) reproducible trials. Agreements of the S/V ratios are within ±3%, and those of reaction rates are within ±2%. The slopes of the plot have R^2 values of 0.9431 and 0.9625, respectively, for the relationships of the rates of disappearance of PA and MA to the S/V ratios.

surface, the same relationship applies to the initial rates for the appearance of the PI, i.e., (+d[PI]/dt).

Additionally, the Pyrex IR gas cell surface was modified by: (1) silation via pretreatment with triethylamine(g) and evacuation of the cell followed by treatment with trimethylchlorosilane-(g);[16a] (2) silation using a solution of trimethylchlorosilane and octadecyltrichlorosilane (1 × 10^{-3} M in CH_2Cl_2);[16b] (3) coating the cell surface with molten paraffin wax; and (4) re-using the paraffin-coated cell, but with new NaCl windows. Further surface modification was achieved by pretreatment of the Pyrex cell with $^2HCl/^2H_2O$, aqueous HCl, sodium methoxide/^2H_2O, and sodium methoxide/H_2O, respectively. Reactions were also run in gold, quartz, and Teflon. Table S1 (Supporting Information) gives data for these surface-modified reactions.

The variations of initial rates under pseudo-first-order conditions, i.e., (−d[PA]/dt) with MA in excess, as a function of initial pressure, are provided in Table S2 (Supporting Information).

Graphical results of the integrated rate equations for zero-, first-, and second-order reaction kinetics for PA (●) and MA (▲) based on the large volume of data obtained at ca. 20 Torr in each reactant are given in Figure S2 (Supporting Information). For the first-order process in PA (Figure S2b, Supporting Information), R^2 = 0.9968, while for the second-order process (Figure S2c, Supporting Information), R^2 = 0.9993. For the first-order process in MA (Figure S2b, Supporting Information), R^2 = 0.9892, while for the second-order process (Figure S2c, Supporting Information), R^2 = 0.9885. Thus, the order does

(14) Suydam, F. H. *Anal. Chem.* **1963**, *35*, 193.

(15) Mascavage, L. M.; Dalton, D. R. *Tetrahedron Lett.* **1991**, *32*, 3461. Coarse porosity Pyrex filters are prepared from granular glass of average diameter particle size between 75 and 105 μm. The density of an average disk is 2.01 gm/cm^3, from which it follows that the average surface area is about 3.3 × 10^2 cm^2/g.

(16) (a) Tripp, C. P.; Hair, M. L. *J. Phys. Chem.* **1993**, *21*, 5693. (b) Tripp, C. P. Private communication.

TABLE 1. Initial Rates (Rate^0) for the Disappearance of 2,2-Dimethylpropanal$_{(g)}$ (Pivaldehyde, PA) and Methanamine$_{(g)}$ (Methylamine, MA) and the Appearance of 2,2-Dimethylpropanal Methylimine$_{(g)}$ (PI) for the Reaction between the Gases PA and MA in Various IR Cells[a]

cell surfaces	P^0 PA (Torr)	P^0 MA Torr	[PA]^0 (10^5 mol)	[MA]^0 (10^5 mol)	rate^0 = -d[PA]/dt (10^6 mol min^{-1})	rate^0 = -d[MA]/dt (10^6 mol min^{-1})	rate^0 = +d[PI]/dt (10^6 mol min^{-1})
Pyrex	2.40	21.74	0.259	2.34	0.837	1.24	0.86
	6.61	21.79	0.826	2.43	1.76	3.04	1.98
	15.03	39.61	1.65	4.22	1.38	2.25	1.55
	39.65	18.71	4.34	2.05	4.50	5.41	2.97
	52.45	16.06	5.74	1.76	2.04	5.55	3.76
	58.24	4.64	6.26	0.49	1.84	8.98	5.19
	14.41	6.19	1.59	0.693	2.02	3.69	2.10
waxed	9.87	13.88	1.09	1.54	0.149	0.180	0.02
	9.84	27.19	1.08	2.98	0.211	0.238	0.03
waxed, used[b]	10.33	14.24	1.15	1.58	0.140	0.174	0.03
	16.57	15.70	1.84	1.74	0.187	0.328[c]	0.16
silated:[d] $Et_3N_{(g)}/CH_3SiCl_{(g)}$	10.66	39.78	1.17	4.26	0.686	1.13	0.78
$(CH_3)_3SiCl_{(l)}/CH_3(CH_2)_{17}SiCl_{3(l)}$	18.09	54.19	1.99	6.00	0.813	1.52	1.05
	17.09	105.94	1.88	11.7	0.872	1.39	0.38
Pyrex, with sidearm[e]	6.38	10.73	0.75	1.26	2.02	2.12	2.09
	19.59	9.59	3.21	1.57	4.08	5.71	5.47
	18.92	41.05	3.08	6.72	5.68	5.82	6.86
	19.68	63.28	3.20	10.37	5.88	5.67	7.15
	39.24	19.77	4.67	2.85	3.80	5.43	6.38
	52.88	18.38	6.18	2.15	4.25	6.15	8.49
Teflon	9.13	11.33	1.91	2.37	0.824	1.47	6.88
	16.25	54.21	3.41	11.4	6.22	11.63	6.82

[a] All reactions were carried out at 295 ± 2 K, in IR cells with sodium chloride windows. The reaction of PA was followed in both the C−H and C═O regions (2720.0−2661.0 and 1782.9−1726.06 cm^{-1}, respectively). Results are within ±1% agreement. The data in the table are for the C═O region. Initial pressures, P^0, are those determined from the first acquired spectrum. Other than reactions in the Pyrex cell with the sidearm, about 60 ± 15 s elapsed between the time the gases were mixed at the vacuum rack and when the first spectrum was acquired. All data are expressed as the average of at least two reproducible replications. See Table S1 (Supporting Information) for data with initial pressures of 20 Torr of each reactant. [b] Formation of imine delayed about 4 min. [c] Overnight, the amount of imine continued to increase, yet no amine remained to react! [d] See the Experimental Section. [e] See Figures S3 and S4 (Supporting Information).

TABLE 2. Initial Rates (Rate^0) and Activation Parameters for the Disappearance of 2,2-Dimethylpropanal$_{(g)}$ (Pivaldehyde, PA) and Methanamine$_{(g)}$ (Methylamine, MA) and the Appearance of 2,2-Dimethylpropanal Methylimine$_{(g)}$ (PI) for the Reaction between the Gases PA and MA, in Pyrex IR cells[a]

	rate^0 = -d[PA]/dt (10^6 mol min^{-1})	rate^0 = -d[MA]/dt (10^6 mol min^{-1})	rate^0 = +d[PI]/dt (10^6 mol min^{-1})
T = 283 K	2.73	3.57	1.75
T = 294 K	3.49	3.92	3.90
T = 331 K	5.55	7.55	5.92
E_a, kcal mol^{-1}	2.66	3.02	4.16
$\Delta H^{\ddagger}_{294}$, kcal mol^{-1}	5.23	6.09	8.98
$\Delta S^{\ddagger}_{294}$, eu mol	−68.99	−68.47	−70.55

[a] All reactions were initially made up at 19.7 ± 0.8 Torr PA$_{(g)}$ and 203 ±3 Torr of MA$_{(g)}$. Temperatures are accurate to ± 0.5 °C. All reactions were carried out in IR cells with sidearms (see Figures S3 and S4 (Supporting Information)) having sodium chloride windows. The reaction of PA was followed in both the C−H and C═O regions (2720.0−2661.0 and 1782.9−1726.06 cm^{-1}, respectively). Results are within ±1% agreement. The data in the table are for the C═O region. All data are expressed as the average of at least two reproducible replications.

not appear to be integral, and the pathways cannot be clearly defined as either first- or second-order despite the increase in rate with increasing concentration. We attribute the involvement of surface in the addition and elimination processes to the presence of nonintegral orders, although simultaneous reactions cannot be ruled out.[17]

Two additional features are worthy of note. First, recognizing that the early work of Schiff [1] demonstrated that *2* equiv of amine might be expected to react with an aldehyde, and being cognizant that transamination processes are recognized as a reaction between amino acid substrate and active-site lysine-coordinated pyridoxal-derived imine (vide infra), we undertook to examine the addition of methanamine (MA$_{(g)}$) to 2,2-dimethylpropanal methylimine (PI$_{(g)}$). Thus, 20 Torr PI$_{(g)}$ in the body of the IR cell was allowed to react with 20 Torr MA$_{(g)}$ at room temperature. Although a very small (ca. 0.5%) increase in [PI] and decrease (also ca. 0.5%) in [MA] was observed in the first 30 min after mixing, no further change occurred on standing, and it is concluded that no reaction occurred. We attribute the small initial change to a desorption of imine and its replacement on the surface by amine.

Second, presuming that initial carbinolamine formation might be examined more closely if elimination to imine were inhibited, initial rate date for the reaction of PA$_{(g)}$ with *N*,*N*-dimethylamine (DA$_{(g)}$) was sought. A reaction mixture initially 20 Torr in each showed considerable scatter in the initial (over the first ca. 3 min) rate data, but for this reaction of DA, plots of [PI]/[PA], [PI]/[DA], and [PA]/[DA] vs time were comparable over a period of ca. 1 week and showed no further indications of the

(17) Rettner, C. T.; Auerbach, D. J. *Science* **1994**, *263*, 365.

SCHEME 2. *erythro*- and *threo*-Carbinolamines Derived from Methylamine (MA) and an Aldehyde [R = CH_3; Acetaldehyde (AA) or R= *t*-Bu; Pivaldehyde (PA)] As Complexed with 0−3 Waters[a]

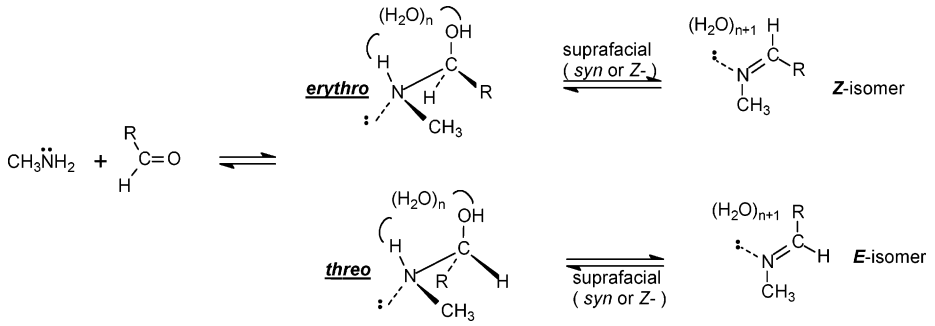

[a] The subsequent elimination to their respective *Z*- and/or *E*-imines generating 1−4 waters is also shown.

TABLE 3. Energies of Activation (kcal/mol) for *erythro*- and *threo*-Carbinolamine Formation and for Elimination to *E*- and *Z*-Imines, Including Dihedral Angles for Elimination

	B3LYP/6-31G(d) [MP2/6-31G(d)]							
transition structures	0W		1W		2W		3W	
AA								
TS-1[a]	*threo*	*erythro*	*threo*	*erythro*	*threo*	*erythro*		
MA + AA to	33.9	33.9	14.3	13.6	12.9	7.8		
carbinolamine	[32.9]	[32.9]	[14.3]	[13.4]	[8.8]	[8.3]		
TS-2[b]	*E*	*Z*	*E*	*Z*	*E*	*Z*	*E*	*Z*
carbinolamine to	51.8	51.1	28.4	31.8	23.8	25.1	25.0	26.0, 28.0
imine	[56.7]	[57.2]	[34.7]	[39.0]	[30.1]	[32.0]	[29.9]	[33.4], [31.1]
H−N−C−OH (deg)	*8.0*	*13.0*	*49.4*	*32.0*	*75.2*	*71.0*	***98.6***	*89.0, 76.8*
PA								
TS-1[a]	*threo*	*erythro*	*threo*	*erythro*	*threo*	*erythro*		
MA + PA to	33.2	33.2	15.1	15.1	10.3	18.1		
carbinolamine	[30.9]	[30.9]	[13.3]	[13.4]	[10.4]	[17.2]		
TS-2[b]	*E*	*Z*	*E*	*Z*	*E*	*Z*	*E*	*Z*
carbinolamine to	50.2	54.7	28.2	29.7	20.6	24.1	20.7	21.5, 26.8
imine	[67.8]	[75.1]	[51.2]	[51.1]	[38.9]	[42.4]	[37.6]	[41.4], [44.2]
H−N−C−OH (deg)	*22.6*	*10.0*	*44.8*	*49.6*	*20.6*	*24.1*	***99.0***	*62.8, 74.2*

[a] **TS-1**: transition state for reactants to carbinolamine. [b] **TS-2**: The transition state for carbinolamine to imine. Structures were optimized at the B3LYP/6-31G(d) level and corrected for zero-point energies scaled by 0.9804. Energies in parentheses represent single-point calculations (MP2/6-31G(d)//B3LYP/6-31G(d)) level corrected with the zero-point energies of the B3LYP geometries.

initially observed scatter. However, most interestingly, the disappearance of *both* reactants and the appearance of the methylimine ($PI_{(g)}$) occurred, but at rates about 2 orders of magnitude less than the reaction of $PA_{(g)}$ with $MA_{(g)}$ under similar conditions. We suggest that exchange of the methyl groups on the walls to produce small quantities of methanamine (MA) may be occurring by a process similar to that recently found in solution.[18]

Computational Results and Discussion

We focused our attention initially on the reaction of MA with AA to give carbinolamine, which can eliminate water forming geometrically isomeric imines. The elimination reactions were formulated with 0−3 water molecules arrayed in cyclic fashion to, presumably, facilitate gas-phase dehydration (Scheme 2; R = CH_3) through amelioration (by delocalization) of whatever charges might form in the processes (Scheme 1).

The computations indicated dramatic reductions in the energy barriers for a concerted elimination when two water molecules bridged the N−H and O−H hydrogens for all of these reactions. Table 3 presents a summary of the potential energy barriers calculated for the addition of MA to AA to form the carbinolamines (*threo*- and *erythro*-*N*-methyl-1-aminoethanol) and for the elimination of water from these intermediates to produce *E*-and *Z*-imines (*N*-methylethanalimine). Results for the reaction of MA with PA were very similar and are also included in Table

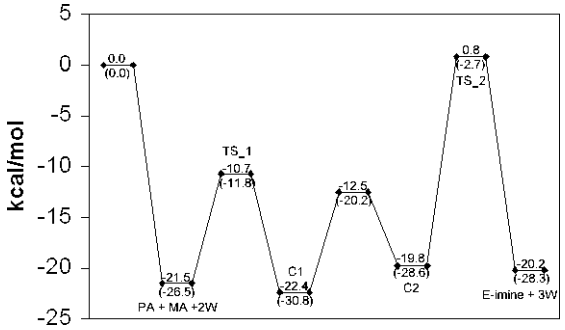

FIGURE 3. Energy profile for the reactions of methanamine (CH_3NH_2, MA) with 2,2-dimethylpropanal (pivaldehyde, $(CH_3)_3CCHO$, PA) and 2 waters ($2H_2O$, 2W) leading to *E*-imine (PI). A figure representing the analogous data for the reaction of MA with AA is available in the Supporting Information (S18, S19). Energies relative to the unassociated reactants at 0.0 kcal/mol are given for structures that are fully optimized at the B3LYP/6-31G(d) level with zero-point energy corrections scaled by 0.9804. Parenthesized values are single point energies at the MP2/6-31G(d) level using the B3LYP geometries and frequency calculations. Data for these figures are given in Table 3. **C1** refers to the carbinolamine formed by reaction of aldehyde with amine; **C2** refers to the carbinolamine structure that leads to elimination of water.

(18) Callahan, B. P.; Wolfenden, R. *J. Am. Chem. Soc.* **2003**, *125*, 310.

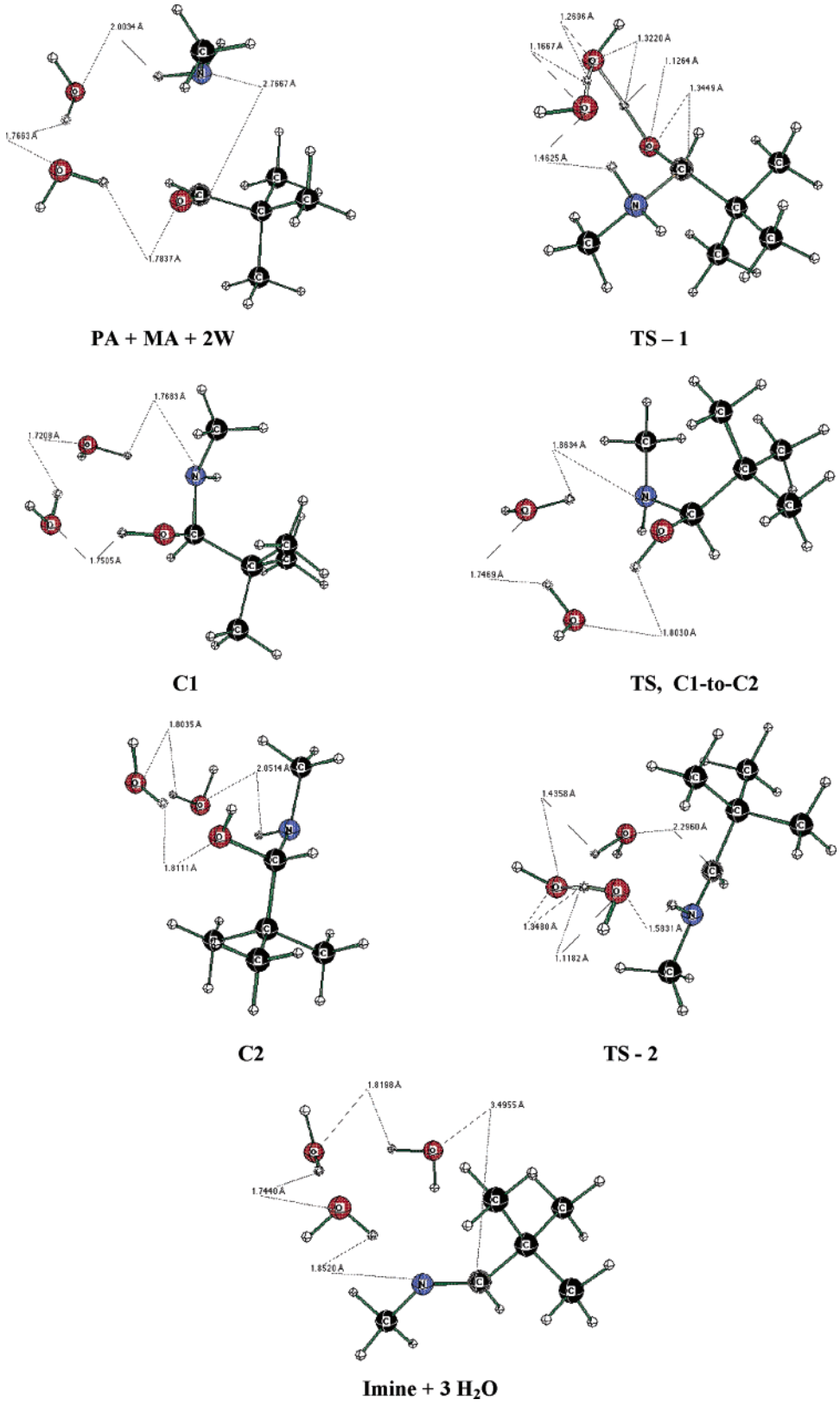

FIGURE 4. Representations of reactants, products, transition states, and intermediates in the reaction between MA + PA + 2 waters (see text).

3. In each case, there is a small subsequent cost for rotation of the initially formed carbinolamine to the rotamer favored for elimination, and this is exemplified for the reaction of MA with PA as illustrated in Figures 3 and 4 for the specific reaction involving two waters (2W). The heights of the two barriers for the transitions, respectively, to carbinolamine and to imine are listed as **TS-1** and **TS-2**. It is clear that transition energies are significantly reduced by incorporation of a single water molecule, and further reduction occurs with a second water molecule.

TABLE 4. Selected Bond Lengths (pm)[a]

structure	N−H	N−C	C−OH
$CH_3NHCH(OH)CH_3$	10.19	14.48	14.38
same + $2H_2O$	10.26	14.23	14.77
TS-2[b]	11.08	13.03	36.78
TS-2 (^{2}H−N)	11.08	13.03	35.55

[a] Carbinolamine, Scheme 2, R = CH_3; B3LYP/6-31G(d). [b] **TS-2**: transition state for carbinolamine to imine.

TABLE 5. Selected Bond Lengths (pm) and Angles (deg) for the reaction of PA with MA As Shown in Figure 4

structure	no. of H_2O	H−N	N−C	C−O	N···C=O
$CH_3NH_2 + (CH_3)_3CCHO$	0	10.19	36.37	12.14	58.5
$CH_3NH_2 + (CH_3)_3CCHO$	2	10.27	27.68	12.25	97.1
TS-1[a]	2	11.23	15.90	13.45	108.7
carbinolamine	0	10.18	14.36	14.43	58.1
carbinolamine[b]	2	10.24	14.25	14.83	65.6
TS-2[c]	2	10.78	12.96	22.95	77.6

[a] **TS-1**: transition state for reactants to carbinolamine. [b] Oriented for elimination to *E*-imine. [c] **TS-2**: transition state for carbinolamine to imine.

Considering the reaction between MA and PA further, it is evident (Figure 3) that considerable energy is released through simple complexation of amine with the aldehyde, and in this process, bond distances are altered from those of the water-free complex in the direction of the transition structure for carbinolamine formation. We examined the two-water-catalyzed dehydration reactions of the carbinolamines derived from condensations of MA with AA and with PA that lead to the respective *E*-imines by an intrinsic reaction coordinate (IRC) routine (see the Supporting Information).[19] The reactions are asynchronous with C−OH bond-breaking preceding rupture of the N−H bond. In concert with this, substitution of ^{2}H for ^{1}H on nitrogen, as illustrated for the reaction of MA with AA, only increases the barrier to dehydration by 0.4 kcal/mol (B3LYP); the deuterium isotope effect is minimal. The ^{2}H−N bond length and the dihedral angle (^{2}H−N−C−OH) remain essentially unchanged with respect to the values for the undeuterated transition structure of the elimination catalyzed by two waters (Table 4).

Specifically, for the reaction of MA with PA, on the way to the carbinolamine, the C−O double bond is lengthened as the amine nitrogen is brought closer to the bond-forming distance. Moreover, the association of the two reactants with water positions the nitrogen at an angle to the carbonyl (N···C=O) that is closer to the optimal approach angle for bond formation (Table 5).

Since it is well appreciated[20] that ammonia and amines readily serve as proton acceptors but not donors, we anticipated that methanamine would not replace water in either carbinolamine formation or its subsequent dehydration. In the event, for the reaction between PA and MA, while it was found that replacing water by methanamine (Table 6) did serve to lower both barriers relative to the absence of either water or amine, the extent of lowering was much less pronounced for the latter.

Reactant structures differing only in the placement of "catalytic" methanamine present a multitude of very similar possibilities from which to start. However, the minima found among them differed by less than 1.5 kcal/mol and thus would not alter the following conclusions: (1) Catalysis by methanamine lowers the barriers to both reactions. (2) The effects are less dramatic than they are with water as catalyst (compare Table 3 data with Table 6). The latter is consistent with the calculations that suggest early stage C−OH bond-breakage; i.e., the more efficient catalyst is the stronger acid. That is, ability to transfer a proton to the C−OH is more critical than ability to serve as a Lewis base and accept the proton from the nitrogen.

TABLE 6. Energies of Activation (kcal/mol) for Methanamine as Proton Donor/Receptor for the Reaction between PA and MA

transition structure[a]	no. of CH_3NH_2	B3LYP[b]		MP2[c]	
to carbinolamine from $CH_3NH_2 + (CH_3)_3CCHO$	0	33.2		30.9	
	1	20−22		18−19	
	2	18.3		16.2	
from carbinolamine to imine, $CH_3N{=}CHC(CH_3)_3$	0	*E*	*Z*	*E*	*Z*
	1	50.2	54.7	67.8	75.1
	2	30.2	32.5	32.3	36.7
	3	32.3	36.5	35.7	41.2
		32.9	32.1	34.8	36.5

[a] Multiple orientations of two or more MA produced different energy minima. An example is provided in the transition structure for one additional MA. Others, not shown, are similar, and the lowest single value found is given. [b] Structures were optimized at the B3LYP/6-31G(d) level and corrected for zero-point energies that had been scaled by 0.9804. Energies were computed from the lowest energy reactant conformation. [c] MP2/6-31G(d)//B3LYP/6-31G(d) with zero-point corrections based upon the frequency calculations associated with the geometry optimizations

Conclusions

Reaction between the gases 2,2-dimethylpropanal and methanamine in an infrared gas cell requires a surface for consummation. The process, which yields imine *N*-(2,2-dimethylpropylidene)methanamine, presumably occurs via the undetected carbinolamine, and water is implicated in the addition and elimination processes.

For both the reaction of MA with AA and MA with PA (Figure 3 and Supplementary Information, S18−S19), barriers for loss of water from the respective carbinolamines to produce the respective imines are considerably higher than those for carbinolamine formation. The patterns of relative energies of activation are the same with respect to the number of added waters. Again, for both reactions, the lowest barrier calculated included two waters (at the B3LYP/6-31G(d) level), although involvement of three waters rather than two produced barriers that were within a few kcalories per mole of the former. Not surprisingly as the number of water molecules increased, the number of saddle points possible for the elimination increased as well. This seems to be due primarily to the increasing number of minor conformational differences in the gross structure of the complexes, and at the level of three waters the dihedral angle for the dehydration was capable of extending beyond 90°, effectively producing the possibility of an *anti* elimination (Table 3).

We conclude, first, that in concert with what has been suggested earlier,[9−12] a favorable construction for a gas-phase reaction of an amine with an aldehyde and for cyclic dehydration of the relevant carbinolamine is that of an eight-membered *syn*-like transition structure in which two proton-transferring catalytic

(19) (a) Gonzalez, C.; Schlegel, H. B. *J. Phys. Chem.* **1990**, *94*, 5523. (b) Gonzalez, C.; Schlegel, H. B. *J. Phys. Chem.* **1989**, *90*, 2154.

(20) Nelson, D. D.; Fraser, G. R.; Klemperer, W. *Science* **1987**, *238*, 1670.

units participate. This is consistent with the activation parameters determined for the surface-catalyzed gas-phase reaction of PA with MA, where $\Delta S^{\ddagger}$ is indicative of a highly ordered transition state.

Second, it seems clear that, to the extent imines are implicated in the reactions of type I aldolases, transaminases, and other enzymes employing the ubiquitous cofactor pyridoxal phosphate, the general pathway for their use follows Schemes 1 and 2. Further, while there is no requirement for a single mechanism in processes yielding similar or identical products,[17] the work described here shows that carbinol formation and subsequent elimination of water to produce imine may use a cyclic pathway involving at least one water molecule and additional hydroxyl functionality.

Experimental Section

Kinetic Methods. Methanamine (MA, methylamine, anhydrous; ≥98%), *N*,*N*-dimethylamine (anhydrous; ≥99%), 2,2-dimethylpropanal (PA, trimethylacetaldehyde, pivaldehyde; 97%), deuterium oxide (^2H_2O, 99.9 atom % ^2H), deuterium chloride (^2HCl, 20 wt % solution in ^2H_2O, 99 atom % ^2H), octadecyltrichlorosilane (90+%), chlorotrimethylsilane (98%), sodium methoxide (powder, 95%), chloroform-*d* ($^2HCCl_3$, 100.0%), hydrochloric acid, and paraffin wax were obtained commercially. The imine, *N*-(2,2-dimethylpropylidene)methanamine (PI), was prepared by the method of Quast and Kees.[13] The methanamine cylinder was attached to the vacuum rack with stainless steel Swagelock fittings, and before use in a reaction, the gas was condensed into a liquid nitrogen trap on the vacuum rack and any noncondensables pumped away. The 2,2-dimethylpropanal was stored in a Pyrex tube equipped with a Teflon- and Kel-F-to-glass stopcock (which was grease free) and attached to the vacuum rack via a 10/30 standard taper joint. It was degassed and further purified using three trap-to-trap distillations to liquid nitrogen from ice water. Vacuum was monitored by a Pirani gauge, and pressure measurements were made using an capacitance bridge manometer with a stainless steel diaphragm (linked to a digital VOM; 1 V = 100 Torr). The manometer was calibrated by measuring the pressure of hydrogen chloride at various temperatures and by freezing known volumes of hydrogen chloride at measured pressures in the vacuum rack into excess standard potassium hydroxide solution and back-titrating with standard acid.

Absorbance spectra (all 2 cm^{-1} resolution) were utilized throughout for the analyses. ^1H NMR spectra were obtained both in the gas phase and in $^2HCCl_3$ at 300 and 500 MHz.

Infrared cells, as seen in Figures S3 and S4 (Supporting Information), were made of Pyrex glass with Teflon- and Kel-F-to-glass stopcocks between the cell, the sidearm, and the standard taper joint for attachment to the vacuum rack. The main body of the cells and the sidearms were nominally 10.0 cm × 1.5 cm i.d. and 10.0 and 1.0 cm i.d., respectively. The Pyrex cell for variable-temperature work was jacketed with coiled copper tubing (1/8 in.) and connected to an electrically heated, circulating water bath whose temperature was maintained within ±0.5 °C of those reported. Polished sodium chloride windows, nominally 25 × 4 mm, were clamped in place over 2.5 mm thick perfluoro elastomer gaskets. Fused silica windows (1 in. diameter × 1/8 in. thick) were used as noted when testing for interference by salt surfaces. A Teflon infrared cell was made by boring a 2 cm diameter hole down the center of a 5 cm diameter (10 cm long) rod of the specified material. Attachment to the vacuum rack was accomplished by threading a Teflon-to-glass stopcock into an appropriately bored hole halfway along the length of the cell. The cell was cleaned with aqua regia, rinsed exhaustively with distilled water, and oven dried at 50 °C, the windows were mounted, and the assembled cell was pumped on at ca.10^{-5} Torr without further heating for 24 h prior to filling. A brass cell was prepared in the same manner as the Teflon cell. It was then electroplated with gold to a thickness of 100 μm. Other Pyrex cells and a quartz cell were made with dimensions of the Pyrex cells discussed above, but without the sidearm.

To evaluate the effects of the walls and added surface, the surface area of the main body of the Pyrex cells was varied. The surface-to-volume ratio was increased about 20-fold by packing the IR cell with Pyrex fritted glass disks (14 × 2 mm; coarse porosity). Organic impurities were removed by (a) cycling the disks through a glass annealing oven and (b) sonication with chromic-sulfuric acids. After thorough washing (including further sonication) with distilled, deionized water, a further sonication with aqua regia followed by exhaustive washing and sonication with distilled, deionized water (no precipitate with acidic silver nitrate) was effected, and two additional annealing oven cycles were performed. Reproducible glass surface (ca. 3.3×10^2 cm^2/g) could be obtained.[15]

Various attempted modifications of the Pyrex IR cell surface were undertaken. In attempts to remove residual surface water, the cell was evacuated, heated to 150−200 °C for 1 h while under vacuum, cooled to room temperature overnight and (1) filled with the desired reactants or (2) pretreated with 50 Torr of methanamine (3 h), evacuated (1 h), and pretreated with 50 Torr of pivaldehyde. Pretreatment of the Pyrex cells with various solutions included, respectively (1) 10 mL of 20% $^2HCl/^2H_2O$ in 120 mL of ^2H_2O; (2) 10 mL concd HCl in 120 mL of H_2O; (3) a saturated solution of sodium methoxide in ^2H_2O; and (4) a saturated solution of sodium methoxide in H_2O. The pretreatment consisted of soaking the cell for 3 h in the solution, sonicating for 3 h, continued soaking overnight, rinsing with deionized H_2O, followed by oven drying. Also, a Pyrex cell was sonicated for 3 h in $^2HCCl_3$, soaked overnight in the $^2HCCl_3$, and dried in a desiccator. Silation of the surface was achieved by two methods: (1) evacuating the cell, pretreating with 50 Torr of *N*,*N*-diethylethanamine [triethylamine, $(CH_3CH_2)_3N$] (1 h), heating the evacuated cell (200 °C; 1 h), cooling, followed by pretreatment with 50 Torr of trimethylchlorosilane [$(CH_3)_3SiCl$] (1 h), evacuating, heating (200 °C; 1 h) and cooling under vacuum overnight;[16a] and (2) immersing the Pyrex cell in a solution of trimethylchlorosilane and octadecyltrichlorosilane (1×10^{-3} M in CH_2Cl_2),[16b] refluxing for 2 h, cooling overnight while immersed, rinsing with toluene followed by deionized water, and oven drying (110 °C). Further surface modification of the Pyrex cells was achieved by (1) coating the cell surface with molten paraffin wax; (2) reusing the paraffin-coated cell, but with new NaCl windows; and (3) pretreating the evacuated Pyrex vessels with small amounts (ca. 20−30 Torr) of each of the reactants separately for at least 3 h, followed by reevacuation of the cell.

The Pyrex cells, without windows and stopcocks, were cycled through a glass annealing oven at 1040 °F for 2 h (a process helpful[21] in removing even strongly adsorbed residues from silica surfaces) prior to assembling. After cooling in a desiccator, new windows were mounted, the stopcocks inserted, and the cell attached to the vacuum rack. Pumping (10^{-5} Torr) with occasional heating (ca. 200 °C) with a hot-air blower was carried out for 24 h prior to filling.

Before beginning a reaction, a background spectrum of the cell was recorded. The sidearm of the cell was then filled to the appropriate overpressure with methanamine (methylamine, MA), the sidearm's stopcock closed, the system reevacuated, the 2,2-dimethylpropanal (pivaldehyde, PA) introduced into the main body of the cell, and the stopcock to the cell closed. The cell was clamped into place in the IR spectrometer (Figure S4, Supporting Information). An initial spectrum of the aldehyde in the main body of the cell was recorded. The stopcock to the sidearm was opened and then closed, and IR spectra were acquired (eight scans each; 2 cm^{-1} resolution) at frequent, fixed-time intervals. Depending upon the

(21) (a) Schmidt, G.; Gruehn, R. *J. Cryst. Growth* **1982**, *57*, 585. (b) Sumner, A. L.; Menke, E. J.; Dubowski, Y.; Newberg, J. T.; Penner, R. M.; Hemminger, J. C.; Wingen, L. M.; Brauers, T.; Finlayson-Pitts, B. J. *Phys. Chem. Chem. Phys.* **2004**, *6*, 604.

particular run, spectra were initially recorded every 15.0−30.0 s. As many as 30 spectra were obtained on each reaction mixture.

Computational Methods. Geometry optimizations for the gas-phase reaction between (a) ethanal (acetaldehyde, CH_3CHO, AA) and methanamine (methylamine, CH_3NH_2, MA) and (b) 2,2-dimethylpropanal [pivaldehyde, $(CH_3)_3CCHO$, PA] and MA were performed using the Becke three-parameter exchange functional[22] coupled to the nonlocal correlation functional of Lee, Yang, and Parr[23] (B3LYP) with the 6-31G(d) basis sets included in the Gaussian 98 suite of computations.[7] Our interest in employing a DFT method was prompted by reports that the results obtained using sufficiently large basis sets produced good agreement with high level ab initio methods and experimental results.[24] Moreover, this particular method has been shown to work well with hydrogen-bonded systems.[25] We note, however, the recent criticisms of Check and Gilbert who point out that this method often underestimates energy values.[26] For comparative purposes, single-point energies using the second-order Møeller−Plesset method (MP2) and the 6-31G(d) basis sets[27] were obtained. Frequency calculations were obtained on the geometry optimized structures (B3LYP) to ensure that a potential energy minimum had been located. The zero-point energies (B3LYP) were scaled as indicated in the tabulated results (vide infra) and were used to correct both sets of calculated energies. Transition-state structures were located using the quasi-Newton synchronous transit method, QST3;[28] a single imaginary frequency confirmed a saddle point. Both the processes of carbinolamine formation and of dehydration of the latter to imine were examined with additional assisting water molecules. In the case of 2,2-dimethylpropanal (pivaldehyde, PA), additional methanamines (methylamine, MA) were incorporated as potential catalysts. Additionally, reactions of ethanal (acetaldehyde, AA) and methanamine (methylamine, MA) specifically employing two waters were subjected to intrinsic reaction coordinate (IRC) following calculations. Additional details for the reaction of MA with PA are provided in the Supporting Information to avoid unnecessary duplication. The two reaction studies were entirely consistent.

Acknowledgment. Presented, in part, at the 228th ACS National Meeting, Philadelphia, PA, August, 2004; ORGN 477. We are pleased to warmly acknowledge our debt to Mr. David Plasket, glassblower extraordinaire, for vacuum rack work and the design and fabrication of infrared cells. Financial support from ExxonMobil, Inc., and the Departments of Chemistry of Arcadia and Temple Universities is gratefully acknowledged.

Note added in proof. The authors appreciate the suggestion that the hydration of isocyanates also involves a minimum of two water molecules, see: Raspoet, G.; Nguyen, M. Y.; McGarraghy, M.; Hegarty, A. F. *J. Org. Chem.* **1998**, *63*, 6867.

Supporting Information Available: Full descriptions of the calculated geometric parameters and energies of all reported species and stationary and imaginary points, Figures S1−S4 and Tables S1 and S2. This material is available free of charge via the Internet at http://pubs.acs.org.

JO052503Z

(22) Becke, A. D. *J. Chem. Phys.* **1993**, *98*, 5648.
(23) Lee, C.; Yang, W.; Parr, R. G. *Phys. Rev.* **1988**, *94*, 6081.
(24) (a) Pratt, L. M.; Khan, I. M. *J. Comput. Chem.* **1995**, *16*, 1068. (b) Gill, P. M. W.; Johnson, B. G.; Pople, J. A.; Frisch, M. J. *Chem. Phys. Lett.* **1992**, *197*, 499. (c) DFT methods: Ziegler, T. *Chem. Rev.* **1991**, *91*, 651. (d) Labanowski, J., Andzelm, J., Eds. *Density Functional Methods in Chemistry*; Springer-Verlag: Berlin, 1991.
(25) Rablen, P. R.; Lockman, J. W.; Jorgensen, W. L. *J. Chem. Phys. A* **1998**, *102*, 3782.
(26) Check, C. E.; Gilbert, T. M. *J. Org. Chem.* **2005**, *70*, 9828.
(27) Saebo, S.; Almlof, J. *Chem. Phys. Lett.* **1989**, *154*, 83.
(28) Ayala, P. A.; Schlegel, H. B. *J. Chem. Phys.* **1998**, *107*, 375.